

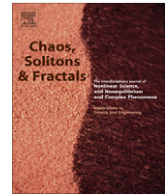


ELSEVIER

Contents lists available at [SciVerse ScienceDirect](http://www.sciencedirect.com)

# Chaos, Solitons & Fractals

Nonlinear Science, and Nonequilibrium and Complex Phenomena

journal homepage: [www.elsevier.com/locate/chaos](http://www.elsevier.com/locate/chaos)

## Spectrum optimization-based chaotification using time-delay feedback control

Jiaxi Zhou, Daolin Xu<sup>\*</sup>, Jing Zhang, Chunrong Liu

State Key Laboratory of Advanced Design and Manufacturing for Vehicle Body, College of Mechanical and Vehicle Engineering, Hunan University, Changsha 410082, PR China

### ARTICLE INFO

#### Article history:

Received 1 November 2011

Accepted 22 February 2012

Available online 22 March 2012

### ABSTRACT

In this paper, a spectrum optimization method is developed for chaotification in conjunction with an application in line spectrum reconfiguration. A key performance index (the objective function) based on Fourier spectrum is specially devised with the idea of suppressing spectrum spikes and broadening frequency band. Minimization of the index empowered by a genetic algorithm enables to locate favorable parameters of the time-delay feedback controller, by which a line spectrum of harmonic vibration can be transformed into a broad-band continuous spectrum of chaotic motion. Numerical simulations are carried out to verify the feasibility of the method and to demonstrate its effectiveness of chaotifying a 2-DOFs linear mechanical system.

© 2012 Elsevier Ltd. All rights reserved.

### 1. Introduction

Chaotification [1,2] (called also chaotization and anti-control of chaos) has drawn the growing attention of many researchers over the last decade, and its engineering applications involve information encryption [3], broadband communication [4], liquid mixing [5]. Recently, an important application for improving the concealment capability of underwater vehicles involves the technique of chaotification that has been employed to blur and disfigure line spectrum emitted from machinery vibration as reported by Yu et al. [6] and Wen et al. [7]. In conclusion, there are two categories of methodology for chaotification, namely synchronization and feedback control.

Synchronization is a collaborative behavior between coupled systems. It includes complete synchronization (CS) [8,9] between two identical systems, and generalized synchronization (GS) [10] between different systems. In engineering practice, CS almost cannot be carried out, since

it is difficult to guarantee that the response system is exactly identical to the drive system. GS without requirement of identical dynamics in master–slave systems is hence usually used to drive a mechanical system chaotic. Based on unidirectional coupling mode of GS, Yu et al. [6] proposed a control scheme to generate or maintain chaos in the nonlinear vibration isolation system (VIS). A chaotic time series generated from a Duffing system was taken as the driving signal, and some parameters of the slave system were defined as a function of chaotic driving signals, and then chaotification in the nonlinear VIS were realized at a particular setting of parameters demonstrated in their numerical example. However, the persistence of chaotification is not guaranteed since this method [6] is sensitive to parameters settings. In a similar way, Wen et al. [7] employed a modified projective synchronization for chaotification where the Duffing system as the master system to drive a nonlinear VIS (response system) chaotic through a control. However, it requires a large control and is seemingly impractical for applications [11].

Another widely used method for chaotification is feedback control. For a stable linear time-invariant and discrete-time system, Wang and Chen [12] designed a

<sup>\*</sup> Corresponding author. Tel./fax: +86 731 8882 1791.

E-mail addresses: [jxizhou@hnu.edu.cn](mailto:jxizhou@hnu.edu.cn) (J. Zhou), [dlxu@hnu.edu.cn](mailto:dlxu@hnu.edu.cn) (D. Xu).

nonlinear feedback controller with tiny amplitude, such as a modulo function of system states. Chaotification is realized by controlling the largest Lyapunov exponent positive meanwhile keeping system states uniformly bounded. Based on this concept, Konishi [13,14] proposed a control method to chaotify a damped linear harmonic oscillator with or without excitation. The key step of this method was to discretize continuous-time systems into discrete-time systems. The discretization was carried out by constructing the map between  $x((n + 1)T)$  and  $x(nT)$  via the integration with respect to the time from  $nT$  to  $(n + 1)T$ , where  $T$  is half of the natural period of the damped oscillator. And then the controller was designed according to Wang and Chen's method [12]. On the contrary, time-delay feedback anti-control of chaos can handle continuous-time systems directly. Wang et al. [1] designed a simple time-delay feedback controller with small amplitude to drive a system chaotic, when the system had an exponentially stable equilibrium point and was controllable. Xu and Chung [15] also pointed out that the time-delay feedback control can be designed as a switch for the choice of system behaviors, namely chaotic or non-chaotic motions. In our previous work [11], the stability of a two degree of freedoms (DOFs) vibration isolation floating raft system with a time-delay feedback control was studied systematically, which gave a guideline of the design of the linear time-delay feedback controller for chaotification. However, to find a set of suitable parameters of the time-delay feedback controller for chaotification, it still relies on bifurcation diagram analysis. From the standpoint of computation efficiency, plotting of a fine-scale bifurcation diagram is very expensive.

In this paper, we attempt to achieve chaotification based on a spectrum optimization method, different from the methods of bifurcation analysis and calculation of the largest Lyapunov exponents. A time-delay feedback controller is introduced due to its useful feature of enhancing system complexity. In the sense of mathematics, a time-delay dynamic system possesses infinite dimensions, makes it much easier to generate chaos even in a first-order linear system [1]. A spectrum performance index will be especially designed in a way of characterizing spectrum spikes and frequency band of the steady state response of a 2-DOFs mechanical system. The genetic algorithm is used for determination of optimal parameters of the time-delay and feedback gain to minimize the index, to which the smaller index corresponds to the result of suppressing spectrum spikes and broadening frequency band, namely chaotification. This approach allows us to easily achieve the chaotification and make a harmonically excited mechanical system be chaotic. Several numerical simulations about the system driven by excitation with different frequencies will be carried out to verify both the feasibility of the spectrum optimization-based chaotification method and the effectiveness of the anti-control of chaos.

It is worthy to note that the existing chaotification methods are only effective on the basis of clearly understanding the system characteristics and under the known conditions. On the contrary, in this paper, the performance index directly characterizes the dynamic behavior based on

the Fourier spectrum of steady state responses, and optimization determines favorable control parameters to minimize the performance index until chaos appears. This enables us to flexibly handle the cases where the system's operational conditions are unknown, or variable, which are typically useful for real applications in system chaotification.

This paper is organized as follow. Section 2 gives the controller design and illustrates the spectrum optimization method. Numerical simulations are carried out in Section 3 to verify the proposed methodology and illustrate the anti-control of chaos in the 2-DOFs mechanical system driven by excitation with different frequencies. Potential engineering applications will be briefly discussed in Section 4. Finally, Section 5 gives some conclusions of the present work.

## 2. Chaotification method

In this section, the time-delay feedback controller will be designed by using Wang and Chen's method [1], and then the spectrum optimization method for chaotification parameters of the controller will be demonstrated. A typical vibration isolation system can be considered as a 2-DOFs mass-spring system [6]. The time-delay feedback control scheme for chaotify the VIS is illustrated in Fig. 1.  $m_1$  and  $m_2$  denotes the isolated equipment and the floating raft, respectively. Both of them are supported by linear springs and linear damping. An actuator is installed between  $m_1$  and  $m_2$  to implement time-delay feedback control for chaotification.

### 2.1. Time-delay feedback controller

The equation of motion of the controlled 2-DOFs system (Fig. 1) can be given by

$$\begin{cases} m_1 \ddot{y}_1 + c_1 (\dot{y}_1 - \dot{y}_2) + k_1 (y_1 - y_2) = F_0 \cos(\omega t) - u(t, \tau) \\ m_2 \ddot{y}_2 + c_2 \dot{y}_2 + k_2 y_2 - c_1 (\dot{y}_1 - \dot{y}_2) - k_1 (y_1 - y_2) = u(t, \tau) \end{cases} \quad (1)$$

where  $u(t, \tau)$  is the time-delay feedback controller. Note that the equation of motion is established in the coordinates  $y$ , whose origins are set at the static equilibrium positions.

By introducing the following parameters for the sake of conveniences

$$\begin{aligned} \omega_{10} &= \sqrt{\frac{k_1}{m_1}}, & \omega_{20} &= \sqrt{\frac{k_2}{m_2}}, & \zeta_1 &= \frac{c_1}{2m_1\omega_{10}}, \\ \zeta_2 &= \frac{c_2}{2m_2\omega_{20}}, & \bar{F}_0 &= \frac{F_0}{m_1}, & \beta &= \frac{m_1}{m_2} \end{aligned} \quad (2)$$

and letting  $\mathbf{z} = [y_1 \ \dot{y}_1 \ y_2 \ \dot{y}_2]^T$ , the equation of motion without the excitation can be re-written as

$$\dot{\mathbf{z}} = \mathbf{Az} + \mathbf{b}\bar{\mathbf{u}} \quad (3)$$

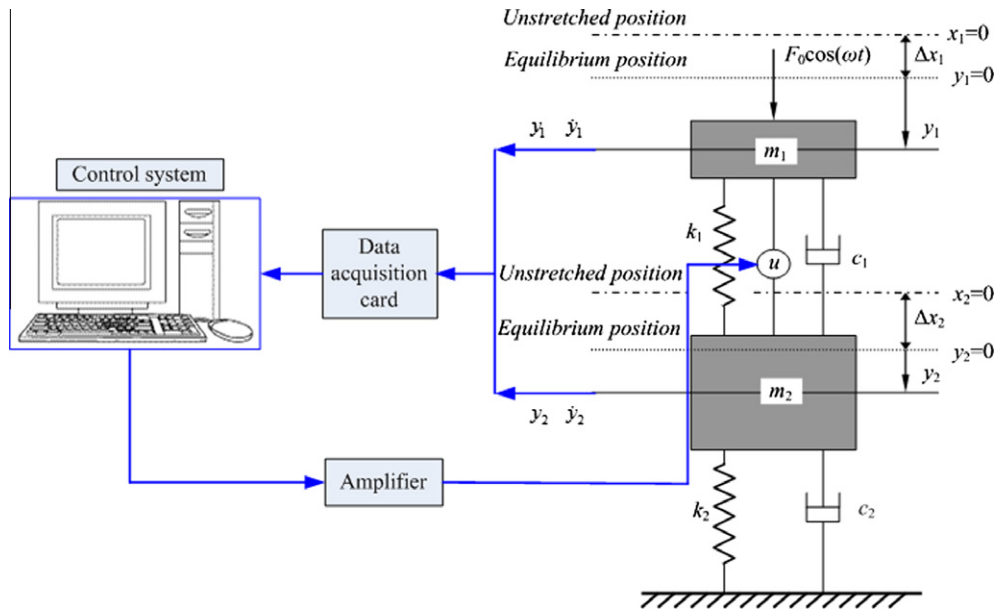


Fig. 1. Schematic diagram of the 2-DOFs system under time-delay feedback control.

where

$$\mathbf{A} = \begin{bmatrix} 0 & 1 & 0 & 0 \\ -\omega_{10}^2 & -2\zeta_1\omega_{10} & \omega_{10}^2 & 2\zeta_1\omega_{10} \\ 0 & 0 & 0 & 1 \\ \beta\omega_{10}^2 & 2\beta\zeta_1\omega_{10} & -\beta\omega_{10}^2 - \omega_{20}^2 & -2\beta\zeta_1\omega_{10} - 2\zeta_2\omega_{20} \end{bmatrix}, \quad (4)$$

$$\mathbf{b} = \begin{bmatrix} 0 \\ -1 \\ 0 \\ \beta \end{bmatrix}$$

and  $\bar{u}(t, \tau) = u(t, \tau)/m_1$ . The system without controller is stable at the equilibrium point (0,0,0,0), which is judged by the Routh–Hrwitz criterion. If the rank of the matrix  $\Theta = [\mathbf{b} \quad \mathbf{A}\mathbf{b} \quad \mathbf{A}^2\mathbf{b} \quad \mathbf{A}^3\mathbf{b}]$  is 4, the system is controllable. According to the linear system theory [16], the system (4) can be reduced to be the controllable canonical form

$$\dot{\mathbf{z}} = \mathbf{A}_c\mathbf{z} + \mathbf{b}_c\bar{u} \quad (5)$$

with the aid of the transformation  $\mathbf{z} = \mathbf{Q}\mathbf{z}$ , where the matrix  $\mathbf{Q}$  is given by

$$\mathbf{Q} = \begin{bmatrix} \mathbf{q}^T \\ \mathbf{q}^T\mathbf{A} \\ \mathbf{q}^T\mathbf{A}^2 \\ \mathbf{q}^T\mathbf{A}^3 \end{bmatrix}^T \quad (6)$$

where  $\mathbf{q}^T$  is the last row of matrix  $\Theta^{-1}$ ; therefore, according to Wang and Chen’s method [1], the time-delay feedback controller can be constructed by

$$u(t, \tau) = f_\tau \sin(\sigma\mathbf{q}^T\mathbf{z}(t - \tau)) \quad (7)$$

$$\mathbf{q} = \left[ -\frac{1}{\omega_{20}^2} \quad \frac{2\zeta_2}{\omega_{20}^3} \quad \frac{4\zeta_2^2 - 1}{\beta\omega_{20}^2} \quad \frac{2\zeta_2}{\beta\omega_{20}^3} \right]^T$$

and written as the sum of displacements and velocities

$$u(t, \tau) = f_\tau \sin \left\{ \bar{\sigma} \left[ -y_1(t - \tau) + \frac{(4\zeta_2^2 - 1)}{\beta} y_2(t - \tau) + 2\zeta_2 \frac{\dot{y}_1(t - \tau)}{\omega_{20}} + 2 \frac{\zeta_2}{\beta} \frac{\dot{y}_2(t - \tau)}{\omega_{20}} \right] \right\} \quad (8)$$

where  $\bar{\sigma} = \sigma/\omega_{20}^2$ .

### 2.2. Spectrum-based performance index and optimization

It is well-known that in frequency domain a harmonic vibration appears to be line spectrum and a chaotic oscillation appears to be a broad-band characteristic [17]. Applying chaotification technique to a mechanical system which is under harmonic excitations, a harmonic vibration could be converted into a chaotic vibration. In view of Fourier spectrum, a line spectrum is converted into a broad-band spectrum. The occurrence of the broad-band spectrum could be very useful to disguise and distort line spectrum signature emitted from machinery vibrations, resulting in the enhancement of concealment capability of underwater vehicles [18].

In the process of chaotification, we attempt a few favorable features. First, we want to broaden the frequency band of the system response as much as possible to eliminate significant line spectra. Second, the peak amplitude of significant line spectrum is expected to be minimized, to reduce line spectrum signals. Bear these in mind, we design a spectrum performance index to represent spectrum configuration, and the controller parameter pair  $(\tau, \sigma)$  is chosen as the design variables. The optimal parameter pair is found to minimize the performance index, and then the controller makes the system chaotic, which is the core idea of the chaotification method in this paper.

The spectrum optimization problem is constructed in the mathematical formulation

$$\begin{aligned}
 &\text{Find}(\tau, \sigma) \\
 &\text{Min. } I = \frac{Y_{\max} - Y_{\min}}{\bar{Y}} \tag{9} \\
 &Y = \sum_{i=1}^N d_i e^{-2\pi j(k-1)(i-1)/N}, \quad k = 1, 2, \dots, N; \\
 &\bar{Y} = \sqrt{\frac{(\|Y\|)^2 - \sum_{i=1}^3 Y_{\max,i}^2}{N-3}}
 \end{aligned}$$

where the objective function is designated by performance index  $I$ , and  $Y$  denotes the discrete amplitudes of the Fourier spectrum, and  $\bar{Y}$  is the root mean square (RMS) that represents the band of frequency region, and  $Y_{\max,i}$ ,  $i = 1, 2, 3$  are the first three largest amplitudes, and  $d_i$  are the discrete data of steady responses (displacements, velocities or accelerations) obtained from experimental measurement or numerical simulations.

This performance index (9) describes a spectrum configuration. The numerator reflects the effect of the difference between the largest amplitude and the smallest one of line spectra and the denominator indicates the other spectrum contribution excluding the first three largest line spectra. To obtain a broad-band spectrum and suppress the most dominant line spectra, it requires a combination of minimizing the quantity  $Y_{\max} - Y_{\min}$  and maximizing the quantity  $\bar{Y}$ . Minimization of the performance index naturally leads to a broad-band spectrum which usually corresponds to a wanted chaotic state. This performance index may be arbitrary but effective, which will be verified in Section 3.1.

Variations of performance index  $I$  against the parameter pair  $(\tau, \sigma)$  are depicted in Fig. 2. The violent fluctuation of the objective function  $I$  against the design variables  $(\tau, \sigma)$  suggests a sensitive dependence and the involvement of strong nonlinearity in optimization process. There are a number of local minima in the search space. By utilizing traditional numerical optimization algorithms [19], such as pattern search and conjugate gradient method, design variables easily fall into local optima, which are strongly dependent on initial guesses. Therefore, genetic algorithm (GA) [19] will be adopted to find the global minimum.

**Table 1**  
System parameters.

Mass $m_1, m_2$	123 kg, 190.5340 kg
Stiffness $k_1, k_2$	$6.3349 \times 10^4$ N/m, $1.0172 \times 10^5$ N/m
Damping factor $\zeta_1, \zeta_2$	0.0089, 0.0163
Excitation frequency $\omega$	Case 1: LF $\omega = 0.3402\omega_{n1} < \omega_{n1}$ Case 2: IF $\omega_{n1} < \omega = 1.7009\omega_{n1} < \omega_{n2}$ Case 3: HF $\omega_{n2} < \omega = 5.1028\omega_{n1}$
Excitation amplitude $F$	50 N
Feedback gain $f_\tau$	5
Time-step, sampling frequency and time span of the RK method	Case 1: LF $T/100, 20\omega,$ 100T Case 2: IF $T/50, 15\omega, 150T$ Case 3: HF $T/25, 10\omega, 200T$

### 3. Numerical examples

The 2-DOFs linear system is driven by a harmonic excitation at three typical frequencies, namely low frequency (LF), intermediate frequency (IF), and high frequency (HF). Parameters of the 2-DOFs linear system and the harmonic excitation are listed in Table 1. Substituting those parameters into the expression of the matrix  $\Theta$  gives

$$\Theta = \begin{bmatrix} 0 & -1 & 0.6625 & 846.8819 \\ -1 & 0.6625 & 846.8819 & -1511.4472 \\ 0 & 0.6456 & -0.9139 & -890.6596 \\ 0.6456 & -0.9139 & -890.6596 & 2134.5224 \end{bmatrix} \tag{10}$$

and the rank of the matrix  $\Theta$  is 4, and hence this system without excitation is controllable. In theory [1], the controller given in Eq. (8) can make the system chaotic.

Two natural frequencies of the system without damping can be written as

$$\omega_{n1,2} = \sqrt{\frac{1}{2}[(1+\beta)\omega_{10}^2 + \omega_{20}^2] \pm \sqrt{\frac{1}{4}[(1+\beta)\omega_{10}^2 + \omega_{20}^2]^2 - \omega_{10}^2\omega_{20}^2}} \tag{11}$$

For three categories of excitation frequencies, Runge–Kutta (RK) integration scheme is utilized to obtain time histories. The time-step, sampling frequency and sampling time are

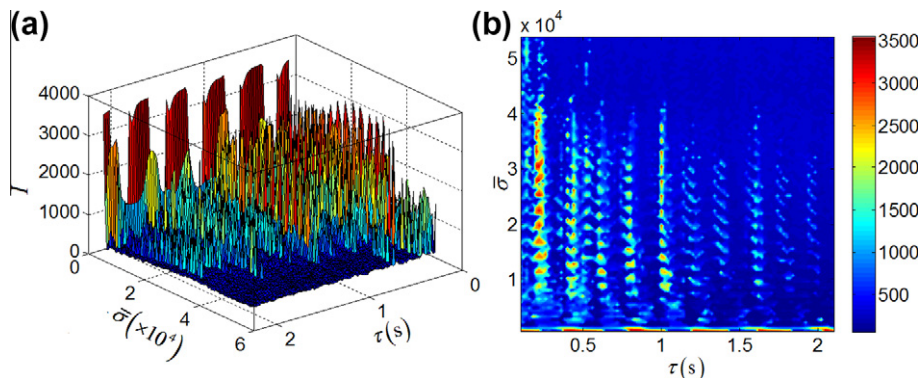


**Fig. 2.** Variations of the performance index against parameter pair  $(\sigma, \tau)$ : (a) 3D plot and (b) filled contour plot with  $\omega = 0.3402\omega_{n1}$ .

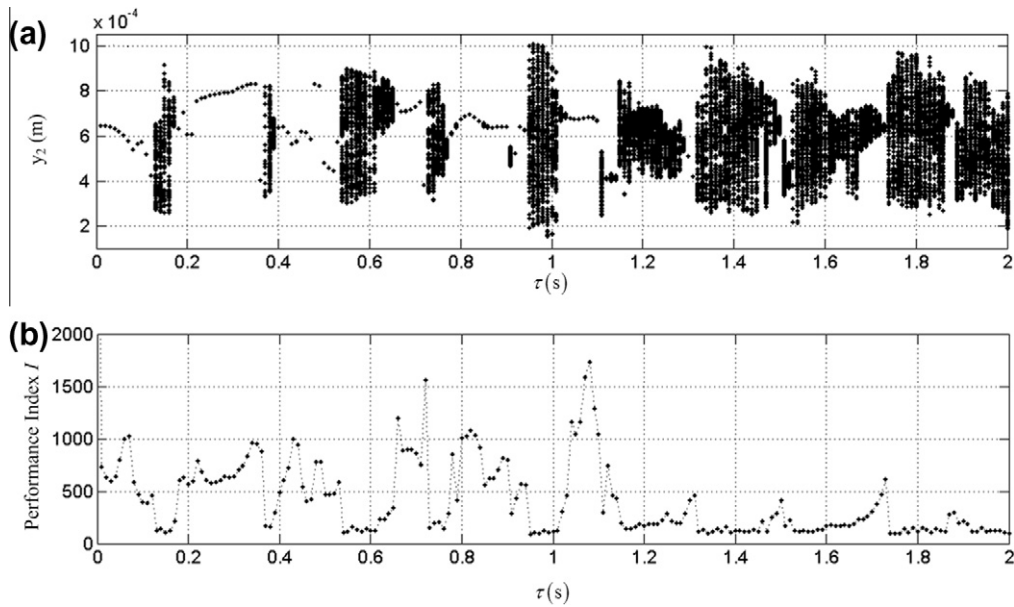


Fig. 3. (a) The performance index  $I$  versus time delay compared with (b) the bifurcation diagram with  $\omega = 0.3402\omega_{n1}$ ,  $\bar{\sigma} = 5338.6692$ .

also given in Table 1, respectively. In addition, the time for dying away the transient response is 200 s. Time histories are obtained by using MATLAB/Simulink®.

### 3.1. Verify feasibility of the performance index

Fig. 3(a) shows a bifurcation diagram that represents the steady state behavior as a function of time delay. Fig. 3(b) shows the variation of the performance index against time delay. Comparing the bifurcation diagram with the performance index, it indicates that the small values of the performance index correspond to chaotic regions in the bifurcation diagram, and the large indices correspond to the non-chaotic oscillations.

Take two typical behaviors as example, namely periodic and chaotic oscillations. Phase portraits and Poincare sections are shown in Fig. 4. Note that a sampling rule for the Poincare sections is to chose  $t_n = nT$ , when the period of the harmonic excitation is  $T$ . The harmonics with higher frequencies than excitation frequency  $\omega$  cannot be demonstrated in Poincare sections. Therefore, there is only one point in Poincare sections (Figs. 4(b) and (c)) for periodic oscillations with high order harmonics. Also seen from Fig. 4 is that case (c) has more harmonic components than case (b). Values of the performance index for these cases are (a) 4157.51, (b) 1728.25, (c) 588.09, and (d) 86.91, respectively. Obviously, the index of chaotic oscillations is smallest but periodic oscillations only having the fundamental harmonic largest, and the index of periodic vibrations with more harmonics is smaller than that with fewer harmonics. Consequently, it can be concluded that the index constructed in this paper is capable of estimating the steady behavior of oscillations, and the small index corresponds to chaotic oscillations. This simple index is arbitrary, but effective. This numerical verification gives

the confidence to perform further design optimization to find out the optimal parameter pair  $(\tau, \sigma)$  for chaotification.

### 3.2. Chaotify the 2-DOFs linear system

The optimal parameter pair is found out by GA for each excitation frequency. GA is a numerical optimization technique based on Darwinian rule, which has been used widely for solving the optimization problem, especially global optimization [19]. For the sake of brevity, details of the genetic programming will not be given in this paper. For this numerical example, the population and maximum generations have been taken as 20 and 100, respectively. In addition, other GA operation parameters have been taken as default values for the function *ga* in MATLAB®. As seen from Fig. 2, most small performance indices are distributed in regions possessing relatively large parameter  $\sigma$ . Furthermore, there exists inherent time delay in the mechanical system with feedback control, and hence it may be more suitable to take relatively large time delay considering the inherent lag. Consequently, the GA search space is determined to be  $1 \leq \tau \leq 3$  and  $5 \times 10^4 \leq \bar{\sigma} \leq 1 \times 10^5$ , and the precision of design variables is set to be 0.01.

#### Case 1: Chaotification at low excitation frequency $\omega = 0.3402\omega_{n1}$

For case 1, the optimal parameter pair is  $(\tau, \sigma)_{opt} = (1.91, 52835.48)$ , and the corresponding performance index is  $I = 273.7093$ . When the time-delay feedback control is absent, the system experiences periodic oscillations, as shown in Fig. 4(a). When the system is controlled by the time-delay feedback with the optimal parameter pair, phase portraits and corresponding Poincare sections as well as Welch power spectral density

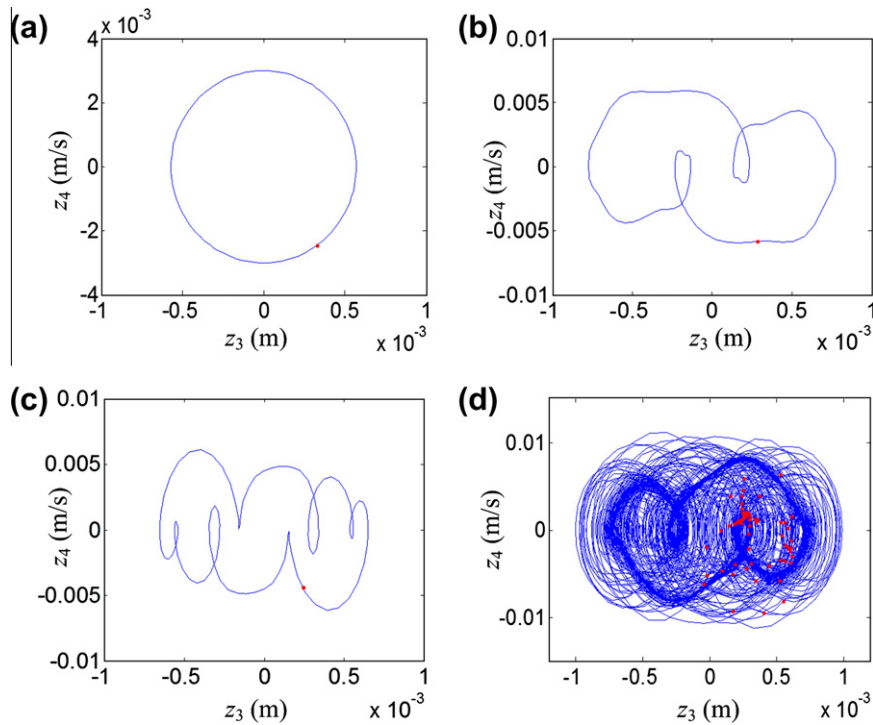


**Fig. 4.** Phase portraits and corresponding Poincare sections: (a)  $\tau=0$ , periodic; (b)  $\tau=1.08$ , periodic with 3 harmonics; (c)  $\tau=0.08$ , periodic with 5 harmonics; (d)  $\tau=0.95$ , chaotic.

(PSD) estimate are plotted in Figs. 5 and 6. It is observed that (1) the trajectory of orbits fills up a section of the phase space, and (2) the power spectrum is continuous, and (3) Poincare sections consist of a collection of unorganized points. From those observations, the motion is likely chaotic. To further diagnose whether the system is chaotic or not, the largest Lyapunov exponent (LE) is calculated by a robust method reported by Rosenstein et al. [20]. The plot of average divergence versus the number of time step  $i$  is shown in Fig. 7. The solid curves are the calculated results with the optimal reconstruction delay  $J=9$  and different embedding dimensions  $m=7, 9, 11$ , and the slope of the dash dot line is the largest LE. It should be noted that the optimal reconstruction delay approximates to the lag where the autocorrelation function drops to  $1 - 1/e$  of its initial value [20], but the selection of embedding dimension may be subjective. The slopes of different  $m$  are almost identical each other, and the largest LE is about 0.1723 ( $J=9, m=9$ ). The positive exponent implies chaotic oscillations [17]. Also seen from Fig. 6(b) is that there exists continuous spectrum in the frequency domain greater than the excitation frequency, besides the line spectrum at the excitation frequency.

*Case 2: Chaotification at intermediate excitation frequency*  
 $\omega = 1.7009\omega_{n1}$ .

For case 2, the optimal parameter pair is  $(\tau, \sigma)_{opt} = (1.32, 50927.24)$ , and the corresponding performance index is  $I = 445.5599$ . The phase portrait and PSD of the controlled system with optimal parameters are

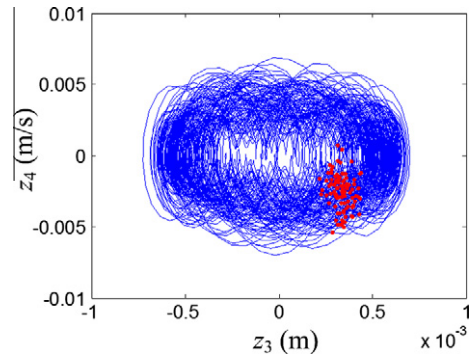


**Fig. 5.** Phase portraits and corresponding Poincare sections of the controlled system with optimal parameter pair driven by the low frequency excitation.

compared with those of the system without control, as demonstrated in Fig. 8. The motion of the system without control is periodic (Fig. 8(a) and (b)). Through observations that Poincare sections (Fig. 8(c)) consist of a cloud of unorganized point and the power spectrum (Fig. 8(d)) is continuous in the region nearby the excitation frequency, as well as the calculation of the largest LE  $\lambda = 0.2183$  ( $J=6, m=9$ ), the motion can be diagnosed to be chaotic.

*Case 3: Chaotification at high excitation frequency*  
 $\omega = 5.1028\omega_{n1}$

For case 3, the optimal parameter pair is  $(\tau, \sigma)_{opt} = (2.22, 87156.62)$ , and the corresponding performance index is  $I = 13.4026$ . The phase portrait and PSD of

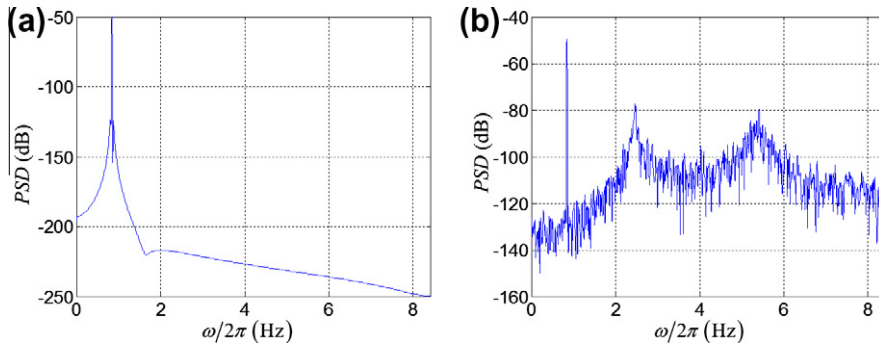


Fig. 6. Power spectral densities (PSD) of the system (a) with and (b) without the time delay feedback control under the low frequency excitation.

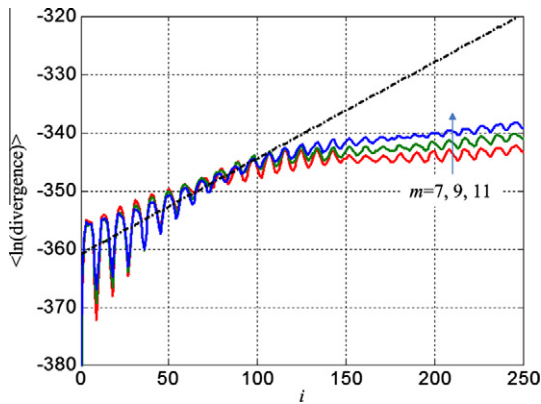


Fig. 7. Plot of average divergence ( $\ln(\text{divergence})$ ) versus the number of time step  $i$ .

the controlled system with optimal parameters are compared with those of the system without control, as shown in Fig. 9. Like cases 1 and 2, without control, the motion is periodic (Fig. 9(a)), and the motion of the controlled system is obviously chaotic, which is detected by phase plane histories, Poincare sections, power spectrum and the largest LE  $\lambda = 1.7506$  ( $J = 14, m = 9$ ), as done in cases 1 and 2. However, the behavior of case 3 is more chaotic than cases 1 and 2, due to the larger LE. It is seen from Fig. 8(d) that the frequency region of continuous spectrum is below the excitation frequency, and a number of sub-harmonics are aroused. Importantly, the line spectrum (Fig. 9(b)) has been changed into the continuous spectrum (Fig. 9(d)).

**Remark 1.** The results of the three typical cases reveal that the spectrum optimization-based chaotification method proposed in this paper is efficient. The spectrum feature has been transformed from a single spike to a broad spectrum. It is of interesting that the continuous spectrum appears in the frequency domain higher than the excitation frequency, when the system is driven by low frequency excitations, and sub-harmonics emerge when harmonic excitations with high frequency. Interestingly, both sub-harmonics and harmonics are aroused while the system excited by intermediate frequency. Unfortunately, the single spike at the excitation frequency cannot be

degraded by chaotification, especially when the excitation frequencies are higher than the second natural frequency or lower than the first natural frequency.

#### 4. Discussion on potential engineering applications

Line spectra emitted from harmonic vibration of machinery systems degrade the concealment of underwater vehicles as this feature signals a strong identity [18]. Lou et al. [18,21] introduced the nonlinear vibration isolation system (VIS) to covert the single frequency input to broad-band chaotic output. However, chaotic oscillations are sensitive to system parameters and excitation conditions, and hence the manufacturing error or variation of excitation conditions will lead to the disappearance of chaotic motion. To reduce the line spectrum, studies about chaotifying the nonlinear VIS have been done by using a method similar to generalized synchronization of chaos [6] and a modified projective synchronization (MPS) method [7]. In Ref. [7], Wen et al. have pointed out that the difficulty for engineering applications of chaotic vibration isolation is how to preserve isolation performance, while to make the VIS chaotic continuously. They achieved the control scheme theoretically based on the MPS method, and the driving singles are generated by a circuit system. However, it requires a large control and is seemingly impractical for applications [11].

The chaotic VIS based on time-delay feedback control with small gain is easily to be carried out, and also possesses capability of driving VIS chaotic and preventing vibratory forces from being transmitted to its base simultaneously. Take the 2-DOFs linear VIS (Fig. 1) as an example, when the damping is neglected, the force transmissibility can be given by

$$Tr = \frac{1}{\left(\frac{\omega_{10}}{\omega_{20}}\right)^2 \left(\frac{\omega}{\omega_{10}}\right)^4 - \left[1 + (1 + \beta) \left(\frac{\omega_{10}}{\omega_{20}}\right)^2\right] \left(\frac{\omega}{\omega_{10}}\right)^2 + 1} \quad (12)$$

which is plotted in Fig. 10. It is observed that, driven by the excitation with frequency  $\omega = 5.1028\omega_{n1}$ , the linear VIS has an excellent performance of vibration isolation. Under the same excitation, the linear VIS is controlled by time-delay feedback with optimal parameters, and then the transmitted force to the base is plotted in Fig. 11, which is compared with the excitation. It is seen that time

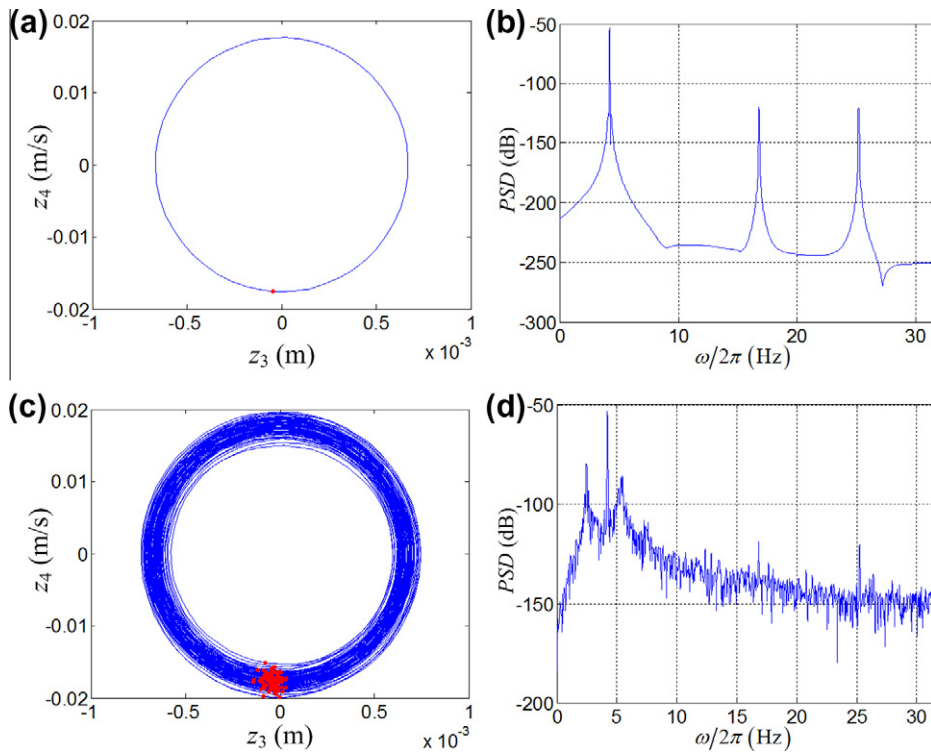


**Fig. 8.** Phase portraits and corresponding Poincaré sections and PSD of the system (a,b) with and (c,d) without time delay feedback control under the intermediate frequency excitation.

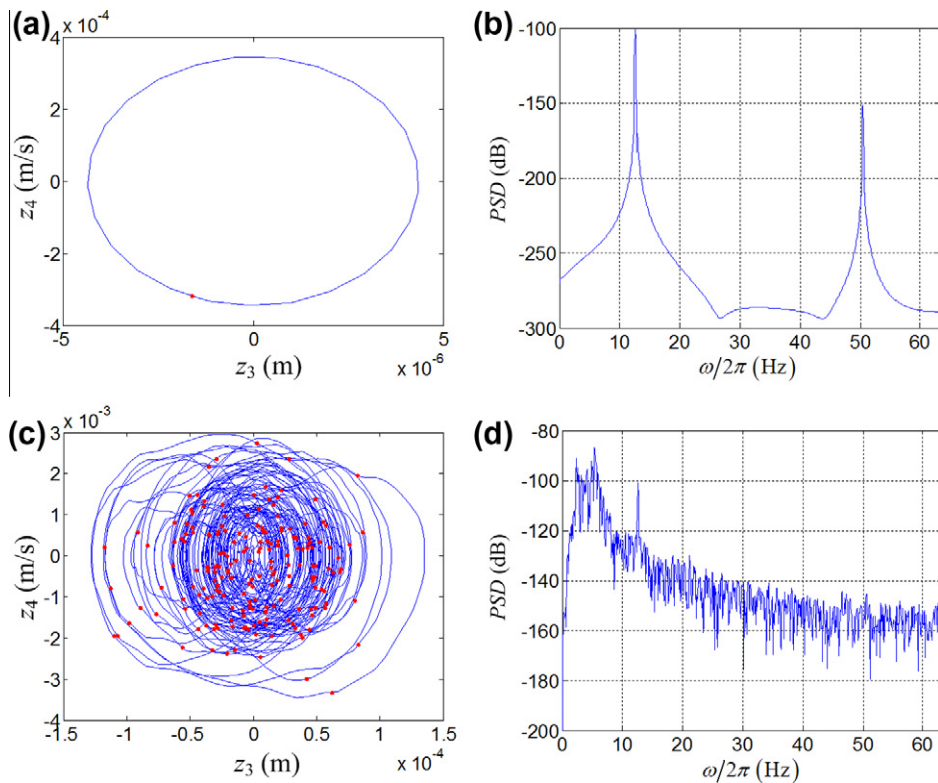


**Fig. 9.** Phase portraits and corresponding Poincaré sections and PSD of the system (a,b) with and (c,d) without time delay feedback control under the high frequency excitation.

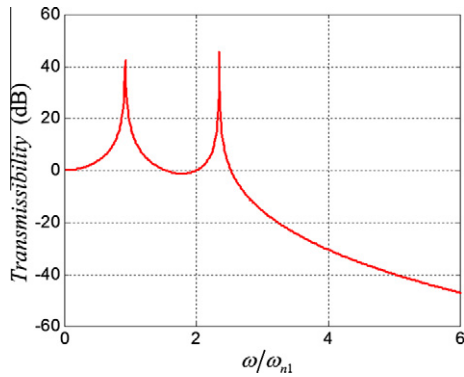


Fig. 10. Transmissibility of the undamped 2-DOFs linear vibration isolation system.

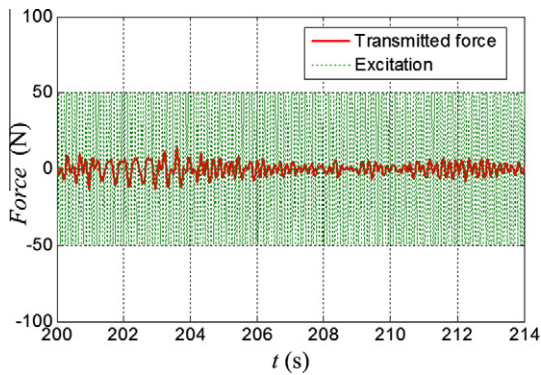


Fig. 11. Excitation with frequency  $\omega = 5.1028\omega_{n1}$  and chaotic transmitted force of the controlled system with optimal parameters.

histories of the transmitted force are chaotic and the amplitude of the transmitted force is much less than that of the excitation. For chaotic oscillations, the force transmissibility has no explicit expression; however, it can be represented in the statistical form, which can be defined as the ratio of root mean square (RMS) of response to that of the excitation [21,22], i. e.

$$Tr_c = 20\log_{10}\left(\frac{RMS(F_T(t_i))}{RMS(F(t_i))}\right) \quad (13)$$

where  $F_T(t_i)$  and  $F(t_i)$  are time histories of the transmitted force and excitation, respectively. In this example, the transmissibility of the chaotic VIS is  $Tr_c = -18.5498$ . It is obvious that  $Tr_c$  is much smaller than zero and larger than  $Tr$ , which demonstrates that the chaotic VIS also has a good performance of vibration isolation, although it is inferior to the linear VIS without control. Nevertheless, we have achieved the key purpose of chaotifying a linear 2-DOFs VIS by time-delay feedback control, reconfigured the spectrum features and remained vibration isolations simultaneously.

Another notable advantage of this chaotification method is reflected in the capability of chaotifying a system by only needing to adjust parameters of the controller to minimize the performance index calculated from steady

state responses, until chaos appears, as earlier mentioned in the Introduction. This allow us to realize the real-time tracking and control when the system with unknown parameters or under variable conditions in practical engineering.

### 5. Conclusions

In this work, a spectrum optimization-based chaotification method in conjunction with time-delay feedback has been proposed to make a 2-DOFs linear mechanical system driven by harmonic excitation chaotic. The nonlinear time-delay feedback controller was employed. Then, a performance index was designed to characterize the Fourier spectrum. Minimization of the performance index generates optimal controlling parameters, i.e. time delay and the parameter  $\sigma$ , which lead to desirable chaotic state. Numerical simulations have verified the feasibility of this method. Results indicate that the 2-DOFs linear system, which is excited by harmonic force with any frequencies, can be driven to be chaotic by the time-delay feedback with optimal parameters, and the potential engineering applications for chaotic vibration isolation is worthy to be expected. The key to this solution is to locate the chaotic parameters by optimization instead of bifurcation diagram that is expensive from the aspect of numerical computations. Note that the method can be easily carried out to chaotify a mechanical system in practical engineering, especially a system with unknown parameters or variable operation conditions, by only adjusting the parameters of controller, according to an optimization algorithm, until the motion become chaotic. The real-time tracking and control for chaotification based on spectrum optimization when the system with unknown parameters or under variable conditions is our future work.

### Acknowledgement

The authors would like to appreciate Professor Shijian Zhu for his offering of modeling parameters of the 2-DOFs linear system. This research work was supported by National Natural Science Foundation of China (11102062,11072075), China Postdoctoral Science Foundation (20100480938), Specialized Research Fund for the Doctoral Program of Higher Education (20110161120040), Fundamental Research Funds for the Central Universities, and the research Grant (71075004) from the State Key Lab of Advanced Design and Manufacturing for Vehicle Body.

### References

- [1] Wang XF, Chen G, Yu X. Anticontrol of chaos in continuous-time systems via time-delay feedback. *Chaos* 2000;10:771–9.
- [2] Fradkov AL, Evans RJ. Control of chaos: methods and applications in engineering. *Ann Rev Control* 2005;29:33–56.
- [3] Fridrich J. Symmetric ciphers based on two-dimensional chaotic maps. *Int J Bifur Chaos* 1998;8:1259–84.
- [4] Hasler M. Engineering chaos for encryption and broadband communication. *Phil T R Soc A* 1995;353:115–26.
- [5] Sharma A, Gupte N. Control methods for problems of mixing and coherence in chaotic maps and flows. *Pramana* 1997;48:231–48.

- [6] Yu X, Zhu S, Liu S. A new method for line spectra reduction similar to generalized synchronization of chaos. *J Sound Vib* 2007;306:835–48.
- [7] Wen G, Lu Y, Zhang Z, Ma C, Yin H, Cui Z. Line spectra reduction and vibration isolation via modified projective synchronization for acoustic stealth of submarines. *J Sound Vib* 2009;324:954–61.
- [8] Pecora LM, Carroll TL. Synchronization in chaotic systems. *Phys Rev Lett* 1990;64:821.
- [9] Mainieri R, Rehacek J. Projective synchronization in three-dimensional chaotic systems. *Phys Rev Lett* 1999;82:3042.
- [10] Rulkov NF, Sushchik MM, Tsimring LS, Abarbanel HDI. Generalized synchronization of chaos in directionally coupled chaotic systems. *Phys Rev E* 1995;51:980.
- [11] Li Y, Xu D, Fu Y, Zhou J. Stability analysis of vibration isolation floating raft systems for chaotification with time-delayed feedback control. *Chaos* 2010;21:033115.
- [12] Wang XF, Chen G. Chaotifying a stable LTI system by tiny feedback control. *IEEE T Circuits-I* 2000;47:410–5.
- [13] Konishi K. Making chaotic behavior in a damped linear harmonic oscillator. *Phys Lett A* 2001;284:85–90.
- [14] Konishi K. Generating chaotic behavior in an oscillator driven by periodic forces. *Phys Lett A* 2003;320:200–6.
- [15] Xu J, Chung KW. Effects of time delayed position feedback on a van der Pol-Duffing oscillator. *Phys D* 2003;180:17–39.
- [16] Kailath T. *Linear systems*. Englewood Cliffs: Prentice-Hall; 1980.
- [17] Moon FC. *Chaotic vibrations: an introduction for applied scientists and engineers*. New York: John Wiley & Sons; 1987.
- [18] Lou J, Zhu S, He L, Yu X. Application of chaos method to line spectra reduction. *J Sound Vib* 2005;286:645–52.
- [19] Venkataraman P. *Applied optimization with MATLAB programming*. New York: John Wiley & Sons; 2002.
- [20] Rosenstein MT, Collins JJ, De Luca CJ. A practical method for calculating largest Lyapunov exponents from small data sets. *Phys D* 1993;65:117–34.
- [21] Lou J, Zhu S, He L, He Q. Experimental chaos in nonlinear vibration isolation system. *Chaos Soliton Fract* 2009;40:1367–75.
- [22] Ravindra B, Mallik AK. Performance of non-linear vibration isolators under harmonic excitation. *J Sound Vib* 1994;170:325–37.